Title	Design and analysis of a new magnetic gear with multiple gear ratios
Author(s)	Chen, M; Chau, KT; Li, WL; Liu, C; Qiu, C
Citation	IEEE Transactions on Applied Superconductivity, 2014, v. 24 n. 3, article no. 501904
Issued Date	2014
URL	http://hdl.handle.net/10722/202869
Rights	IEEE Transactions on Applied Superconductivity. Copyright © IEEE.

Design and Analysis of a New Magnetic Gear With Multiple Gear Ratios

Mu Chen, K. T. Chau, *Fellow, IEEE*, Wenlong Li, Chunhua Liu, and Chun Qiu

***Abstract*—This paper proposes a new magnetic variable gear which offers different speed ratios. In order to provide the gear-ratio-changing ability, a high-remanence low-coercivity permanent magnet (PM), namely the aluminum–nickel–cobalt (Alnico), is utilized. By incorporating the concept of the magnetic gear and the concept of memory machine, a new double-deck structure of the stationary ring is developed to locate the magnetizing winding which can dynamically magnetize or demagnetize the Alnico PM. By using finite element analysis, the electromagnetic performance of the proposed magnetic gear at different gear ratios is analyzed. Hence, the corresponding validity can be verified.**

***Index Terms*—Alnico, finite element method, magnetic gear, memory machine, permanent magnet (PM), variable gear ratio.**

I. Introduction

MECHANICAL gears and gearboxes, which play important roles in vehicular transmission systems, inherently suffer from the drawbacks of high transmission loss, bulky size, annoying noise and wear-and-tear [1], [2]. Magnetic gears can readily supersede mechanical gears because they offer the advantages of physical isolation, maintenance free, silent operation and inherent overload protection [3]–[5]. They can also be integrated into electric machines to further improve the torque density [6], [7]. However, the gear ratio of magnetic gears cannot be adjusted, whereas the gear ratio of mechanical gears can be flexibly varied via the gearboxes for different driving requirements and road conditions.

Although the rare-earth permanent magnet (PM) materials such as neodymium-iron-born (NdFeB) and samarium-cobalt (SmCo) are widely adopted for magnetic gears, there is an increasing concern on the price and supply of the rare-earth elements. Particularly, the use of non-rare-earth aluminum-nickel-cobalt (Alnico) PM material takes the merit of higher cost-effectiveness than the NdFeB PM material for magnetic gears [8]. Recently, by purposely employing the low coercivity of the Alnico PM material, the memory machines [9] can be dynamically magnetized or demagnetized to flexibly vary the air-gap flux density, hence achieving wide constant-power speed range.

The purpose of this paper is to present a new magnetic variable gear for vehicular transmission by combining the concept of magnetic gears and the concept of memory machines. The key is to propose a new double-deck structure of the stationary ring in such a way the magnetizing windings can be artfully inserted to dynamically magnetize or demagnetize the Alnico PM pieces in the outer and inner rotors. By using finite element analysis, the electromagnetic performance of the proposed magnetic variable gear at different gear ratios is analyzed and simulated. Hence, the corresponding validity can be verified.

Manuscript received July 15, 2013; accepted November 12, 2013. Date of publication November 20, 2013; date of current version December 5, 2013. This work was supported by a grant (Project No. HKU 710612E) from the Research Grants Council, Hong Kong Special Administrative Region, China.

The authors are with Department of Electrical and Electronic Engineering, The University of Hong Kong, Pokfulam, Hong Kong (e-mail: ktchau@eee.hku.hk).

Color versions of one or more of the figures in this paper are available online at http://ieeexplore.ieee.org.

Digital Object Identifier 10.1109/TASC.2013.2291972

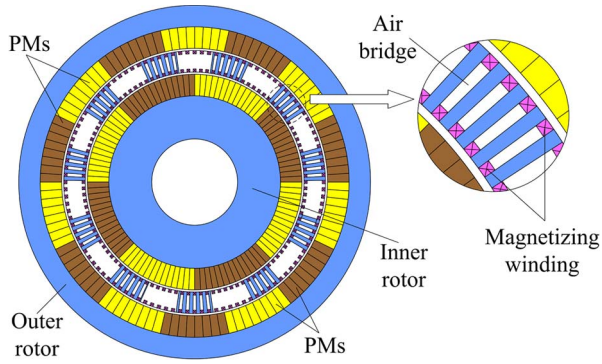

Fig. 1. Configuration of proposed magnetic variable gear.

II. Configuration and Design Principle

The basic configuration of the proposed magnetic variable gear consists of the outer rotor mounted with PM pieces, the double-deck stationary ring with magnetizing windings, and the inner rotor mounted with PM pieces. As shown in Fig. 1, the outer rotor adopting a larger number of PM pole-pairs (7 pole-pairs) operates at a lower speed, whereas the inner rotor adopting a smaller number of PM pole pairs (4 pole-pairs) operates at a higher speed. The double-deck stationary ring functions to modulate the fluxes between the outer and inner rotors. The key design parameters of this magnetic variable gear are listed in Table I.

First, in order to magnetize the inner-rotor and outer-rotor PM poles independently, the double-deck structure of the stationary ferromagnetic ring is proposed. Since the magnetizing winding only needs to carry a temporary current pulse to magnetize or demagnetize PMs, it can be easily embedded into the stationary ferromagnetic ring. The magnetizing winding located in the upper-deck is used to magnetize or demagnetize the outer-rotor PM poles, while the magnetizing winding in the lower-deck is responsible for the inner-rotor PM poles. Small air bridges are purposely incorporated between the upper-deck and lower-deck in such a way that the coils of the two decks

TABLE I
KEY DATA OF PROPOSED MAGNETIC VARIABLE GEAR

Items	Value
No. of pole-pairs in outer rotor	7
No. of pole-pairs in inner rotor	4
No. of iron segments of stationary ring	11
No. of PM pieces in inner, outer rotor	112
No. of upper-deck, lower deck magnetizing winding	112
Thickness of PMs in both rotors [mm]	10
Length of inner, outer airgap [mm]	1.0
Outside radius of outer rotor [mm]	102
Inside radius of outer rotor [mm]	72
Outside radius of inner rotor [mm]	40
Inside radius of inner rotor [mm]	20
Thickness of stationary ring [mm]	10

TABLE II
PM MATERIAL COMPARISON

PM type	B_r(T)	T_c(°C)	H_c(kA/m)
Alnico	0.6-1.4	700-860	40-140
NdFeB	1.0-1.4	310-400	750-2000
SmCo	0.8-1.1	720	600-2000
Ferrite	0.2-0.4	450	120-300

have their individual flux paths and can be excited independently.

Secondly, the Alnico PM material, which has the characteristics of high remanence and low coercivity, is adopted in the proposed magnetic variable gear to obtain the function of dynamic magnetization. The Alnico PM is seldom used in electric machines for industrial applications because its inherent low coercivity may cause accidental demagnetization due to the armature current field. Nevertheless, the proposed magnetic variable gear positively utilizes this drawback to effectively perform gear-changing. Most importantly, since there is no armature current involved in the proposed magnetic variable gear during normal operation, the accidental demagnetization of the Alnico PM is totally eliminated. While the Alnico PM offers the definite advantage of using non-rare-earth elements, it possesses higher Curie temperature than other PM materials, which is essential when working at harsh vehicular environment. Table II gives a comparison of natural properties among different PM materials.

The key design criterion of the proposed magnetic variable gear is the selection of the number of inner-rotor PM pole-pairs N_i, the number of inner-rotor PM pieces N_{mi}, the number of outer-rotor PM pole-pairs N_o, the number of outer-rotor PM pieces N_{mo}, the number of stationary ring segments N_s, the number of the upper-deck magnetizing winding N_{uw} and the number of lower-deck magnetizing winding N_{lw}. According to the magnetic gear operating principle, N_i, N_o, and N_s are governed by:

$$N_s = N_i + N_o \tag{1}$$

$$G_r = \frac{N_o}{N_i} \tag{2}$$

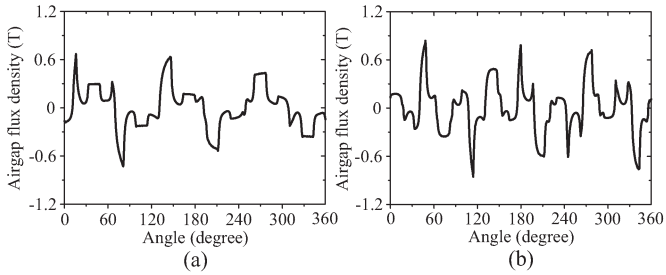

Fig. 2. Airgap flux density waveforms under $G_r = 8/3$. (a) Inner airgap. (b) Outer airgap.

where G_r is defined as the gear ratio.

Initially, N_s is kept constant. In order to vary N_i and N_o, various numbers of PM pieces are properly magnetized or demagnetized to implement various numbers of pole-pairs, so-called the pole-changing ability. The necessary least number of PM pieces for the magnetic variable gear can be defined as:

$$M_1 = \begin{pmatrix} m_{11} & m_{12} & m_{1k} & \dots & m_{1(N_s-1)} \end{pmatrix} \tag{3}$$

where m_{1k} is the least number of PM pieces of one possible gear ratio which is calculated from the least common multiple of $N_s - k$ and k as given by:

$$m_{1k} = [N_s - k, k] \quad k = 1, 2, 3, \dots, (N_s - 1). \tag{4}$$

Then, the possible values of N_{mi}, N_{mo}, N_{uw}, and N_{lw} are determined by:

$$N_{mi} = N_{mo} = N_{uw} = N_{lw} = 2n[\underbrace{m_{1j}, \quad \dots \quad m_{1y}}_{selected\ gear\ ratios}]$$

$$n = 1, 2, 3, \dots \qquad \mathrm{j}, y = 1, 2, \dots, (N_s - 1). \tag{5}$$

Considering the practicability of proposed magnetic variable gear, N_{mi}, N_{mo}, N_{uw}, and N_{lw} should be close to $2n[m_{1j}, \dots m_{1y}]$.

III. PERFORMANCE ANALYSIS

By using finite element analysis, electromagnetic performances of the proposed magnetic variable gear are simulated. The outer rotor of the gear is coupled with the engine and the inner rotor of the gear serves as the output terminal. According to above design principle, the parameters N_{uw}, N_{lw}, N_{mo}, and N_{mi} are all set as 112, and N_s is set as 11.

The airgap flux density waveforms and the resulting torque characteristics of the proposed magnetic variable gear under six sets of G_r are simulated. Namely, the waveforms and characteristics under $G_r = 8/3$, $G_r = 7/4$, $G_r = 6/5$, $G_r = 5/6$, $G_r = 4/7$, and $G_r = 3/8$ are depicted in Figs. 2–13, respectively. The first three sets of G_r are to scale up the engine speed, whereas the last three sets are to scale down the engine speed.

From the airgap flux density waveforms, it can be observed that the inner-airgap pole-pair number and the outer-airgap pole-pair number can be changed according to the gear ratios. Hence, the engine torque or speed (namely the outer-rotor torque or speed) can be scaled down or up accordingly to fulfill

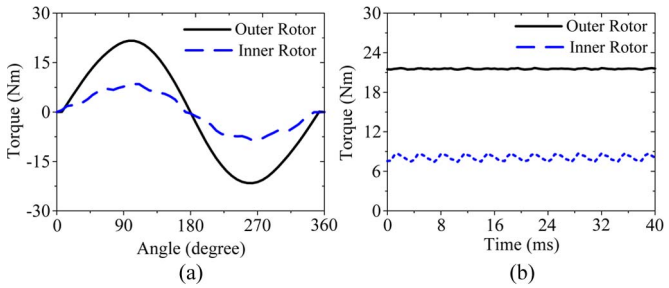

Fig. 3. Torque characteristics under $G_r = 8/3$. (a) Static torque. (b) Steady-state torque.

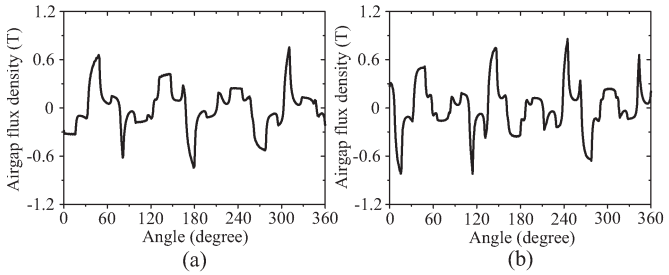

Fig. 4. Airgap flux density waveforms under $G_r = 7/4$. (a) Inner airgap. (b) Outer airgap.

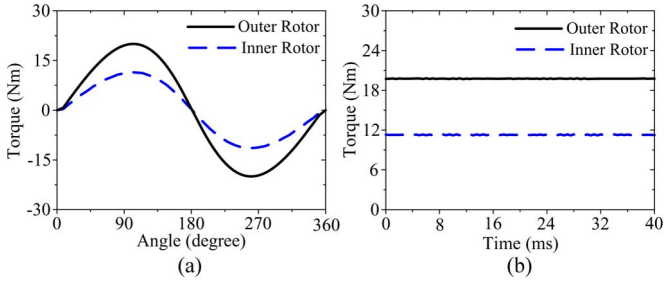

Fig. 5. Torque characteristics under $G_r = 7/4$. (a) Static torque. (b) Steady-state torque.

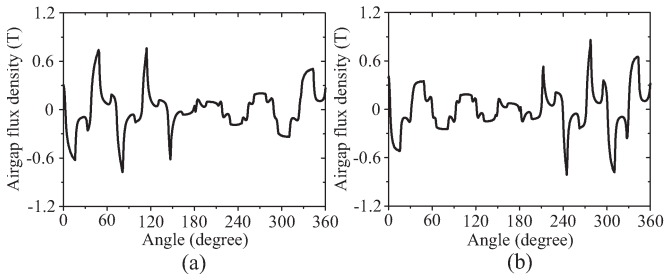

Fig. 6. Airgap flux density waveforms under $G_r = 6/5$. (a) Inner airgap. (b) Outer airgap.

the torque or speed demand at the output shaft (namely the inner-rotor torque or speed).

From the torque characteristics, it can be deduced that the steady-state torque developed at the outer rotor and inner rotor are 21.6 Nm and 8.1 Nm, respectively, under $G_r = 8/3$. The corresponding torque ripples can be calculated as given by 1.1% and 16.1%, respectively. Consequently, the steady-state torques and the torque ripples under other sets of $G_{\rm r}$ can similarly be deduced. All these data are listed in Tables III and IV. It can be observed that the relationship between the torques developed

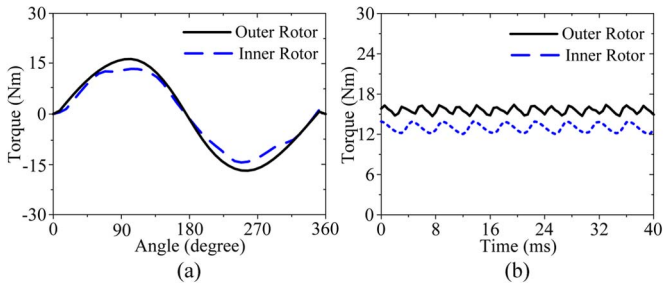

Fig. 7. Torque characteristics under $G_r = 6/5$. (a) Static torque. (b) Steady-state torque.

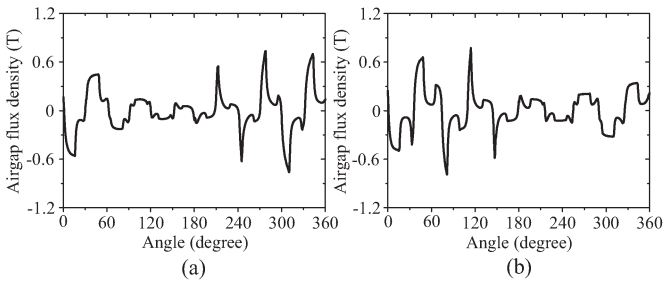

Fig. 8. Airgap flux density waveforms under $G_r = 5/6$. (a) Inner airgap. (b) Outer airgap.

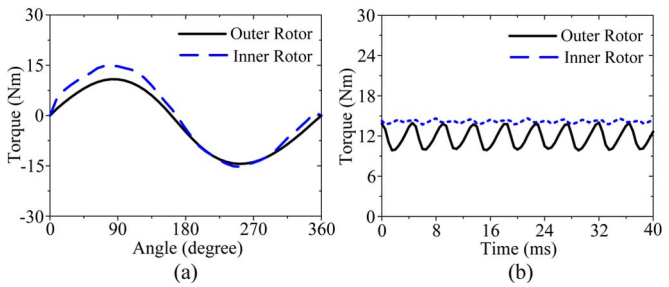

Fig. 9. Torque characteristics under $G_r = 5/6$. (a) Static torque. (b) Steady-state torque.

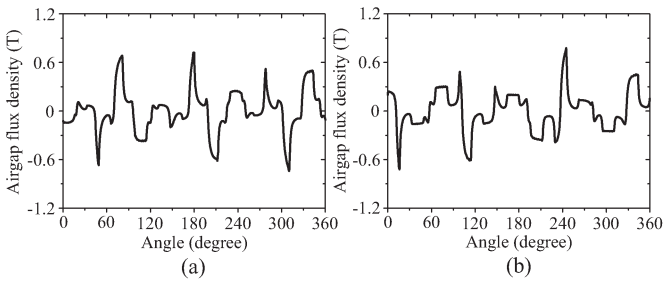

Fig. 10. Airgap flux density waveforms under $G_r = 4/7$. (a) Inner airgap. (b) Outer airgap.

at the outer rotor and inner rotor agrees with the value of gear ratios. For instance, the torque reduction from the outer-rotor torque of 21.6 Nm to the inner-rotor torque of 8.1 Nm is 2.67 which agrees well with the gear ratio of 8/3.

With the six workable gear ratios of the proposed magnetic variable gear, namely from 2.67 to 0.38, the vehicle can readily adjust the gear ratio to fulfill different road conditions and driving requirement. It should be noted that the dynamic magnetization or demagnetization of the Alnico PM can be achieved

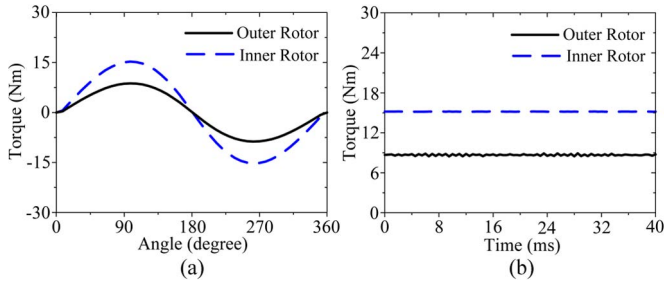

Fig. 11. Torque characteristics under $G_r = 4/7$. (a) Static torque. (b) Steady-state torque.

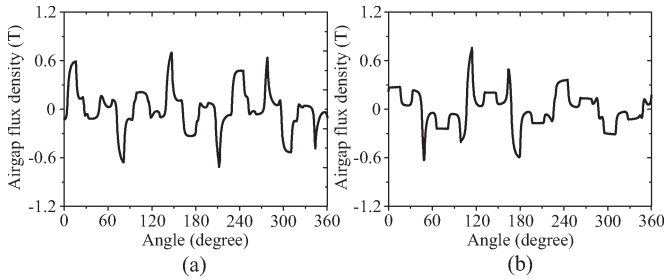

Fig. 12. Airgap flux density waveforms under $G_r = 3/8$. (a) Inner airgap. (b) Outer airgap.

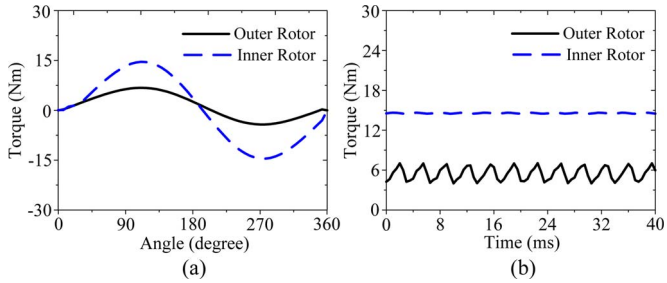

Fig. 13. Torque characteristics under $G_r = 3/8$. (a) Static torque. (b) Steady-state torque.

by applying a positive or negative current pulse with a duration of only 1 ms. The associated power consumption for such gear changing is insignificant.

Finally, it can be observed that the torque ripples developed at the outer rotor are generally more significant than that at the inner rotor, especially under $G_r = 5/6$ and $G_r = 3/8$. This drawback can be alleviated by further increasing the number of PM pieces or optimizing the arc shapes and dimensions. Nevertheless, since the outer rotor is coupled with the engine, the corresponding torque ripple is not so stringent as compared with that of the inner rotor which is used to drive the mechanical load.

IV. Conclusion

This paper has presented a new magnetic variable gear which can provide controllable gear ratios for vehicular transmission. The key is to incorporate the concept of memory machines into the concept of magnetic gears in such a way that the PM pole-pair numbers of the inner and outer rotors can be independently and flexibly controlled. While the Alnico PM material is utilized to perform the desired dynamic magnetization or demagnetization, it takes the definite advantages of using non-rare-earth elements and possessing high Curie temperature. The key design criterion of the proposed magnetic variable gear has been discussed, namely the selection of the number of inner-rotor PM pole-pairs, the number of inner-rotor PM pieces, the number of outer-rotor PM pole-pairs, the number of outer-rotor PM pieces, the number of stationary ring segments, the number of the upper-deck magnetizing winding and the number of lower-deck magnetizing winding. The analysis and simulation results confirm that the proposed magnetic gear can offer six different gear ratios, namely from 2.67 to 0.38, which can readily enable the vehicle adjusting the gear ratio to fulfill different road conditions and driving requirements.

TABLE III
Steady-State Torque Performance

Gear ratio	Inner-rotor torque	Outer-rotor torque
8/3	8.1 Nm	21.6 Nm
7/4	11.3 Nm	19.8 Nm
6/5	13.0 Nm	15.6Nm
5/6	14.2 Nm	12.0 Nm
4/7	15.2 Nm	8.7 Nm
3/8	14.6 Nm	5.5 Nm

TABLE IV
Torque Ripple Performance

Gear ratio	Inner-rotor torque ripple	Outer-rotor torque ripple
8/3	16.1%	1.1%
7/4	1.2%	0.7%
6/5	14.2%	10.8%
5/6	6.5%	34.3%
4/7	0.3%	5.1%
3/8	1.0%	54.5%

References

[1] K. Atallah and D. Howe, "A novel high-performance magnetic gear," *IEEE Trans. Magn.*, vol. 37, no. 4, pp. 2844–2846, Jul. 2001.
[2] L. Jian, K. T. Chau, Y. Gong, J. Z. Jiang, C. Yu, and W. Li, "Comparison of coaxial magnetic gears with different topologies," *IEEE Trans. Magn.*, vol. 45, no. 10, pp. 4526–4529, Oct. 2009.
[3] E. Gouda, S. Mezani, L. Baghli, and A. Rezzoug, "Comparative study between mechanical and magnetic planetary gears," *IEEE Trans. Magn.*, vol. 47, no. 2, pp. 439–450, Feb. 2011.
[4] L. Jian, K. T. Chau, W. Li, and J. Li, "A novel coaxial magnetic gear using bulk HTS for industrial applications," *IEEE Trans. Appl. Supercond.*, vol. 20, no. 3, pp. 981–984, Jun. 2010.
[5] W. Li, K. T. Chau, and J. Li, "Simulation of a tubular linear magnetic gear using HTS bulks for field modulation," *IEEE Trans. Appl. Supercond.*, vol. 21, no. 3, pp. 1167–1170, Jun. 2011.
[6] K. T. Chau, D. Zhang, J. Z. Jiang, C. Liu, and Y. J. Zhang, "Design of a magnetic-geared outer-rotor permanent-magnet brushless motor for electric vehicles," *IEEE Trans. Magn.*, vol. 43, no. 6, pp. 2504–2506, Jun. 2007.
[7] X. Li, K. T. Chau, M. Cheng, and W. Hua, "Comparison of magnetic-geared permanent-magnet machines," *Progr. Electromagn. Res.*, vol. 133, pp. 177–198, 2013.
[8] M. Chen, K. T. Chau, W. Li, and C. Liu, "Development of non-rare-earth magnetic gears for electric vehicles," *J. Asian Elect. Veh.*, vol. 10, no. 2, pp. 1607–1613, Dec. 2012.
[9] F. Li, K. T. Chau, C. Liu, J. Z. Jiang, and W. Y. Wang, "Design and analysis of magnet proportioning for dual-memory machines," *IEEE Trans. Appl. Supercond.*, vol. 22, no. 3, p. 4905404, Jun. 2012.